PROCEEDINGS OF SPIE

SPIEDigitalLibrary.org/conference-proceedings-of-spie

Laser beam propagation through turbulence and adaptive optics for beam delivery improvement

Nicolas, Stephane

Stephane Nicolas, "Laser beam propagation through turbulence and adaptive optics for beam delivery improvement," Proc. SPIE 9641, Optics in Atmospheric Propagation and Adaptive Systems XVIII, 96410B (8 October 2015); doi: 10.1117/12.2194336

SPIE.

Event: SPIE Remote Sensing, 2015, Toulouse, France

Downloaded From: https://www.spiedigitallibrary.org/conference-proceedings-of-spie on 03 Mar 2021 Terms of Use: https://www.spiedigitallibrary.org/terms-of-use

Laser beam propagation through turbulence and adaptive optics for beam delivery improvement

Stephane Nicolas
Norwegian Defence Research Establishment (FFI), Instituttveien 20, 2007 Kjeller, Norway

ABSTRACT

We report results from numerical simulations of laser beam propagation through atmospheric turbulence. In particular, we study the statistical variations of the fractional beam energy hitting inside an optical aperture placed at several kilometer distance. The simulations are performed for different turbulence conditions and engagement ranges, with and without the use of turbulence mitigation. Turbulence mitigation is simulated with phase conjugation. The energy fluctuations are deduced from time sequence realizations. It is shown that turbulence mitigation leads to an increase of the mean energy inside the aperture and decrease of the fluctuations even in strong turbulence conditions and long-distance engagement. As an example, the results are applied to a high energy laser countermeasure system, where we determine the probability that a single laser pulse, or one of the pulses in a sequence, will provide a lethal energy inside the target aperture. Again, turbulence mitigation contributes to increase the performance of the system at long-distance and for strong turbulence conditions in terms of kill probability. We also discuss a specific case where turbulence contributes to increase the pulse energy within the target aperture. The present analysis can be used to evaluate the performance of a variety of systems, such as directed countermeasures, laser communication, and laser weapons.

Keywords: Laser beam propagation, Beam delivery, turbulence mitigation, infrared countermeasures, simulations, numerical model, high-energy laser.

1. INTRODUCTION

Laser beams can be made highly directional, allowing delivery of high power or pulse energy on remote targets. This property has led to an extensive use of lasers in modern warfare, e.g. in designators for laser-guided missiles and bombs, illuminators, rangefinders, directed infrared countermeasures, laser weapons [1;2], and in free-space laser communication links [3].

The performance of laser systems is affected by the natural atmospheric turbulence, and any kind of turbulence induced by the carrier platform, for example the aircraft plume, aero-optical effects, and helicopter rotor downwash. Turbulence causes beam wander, beam broadening, and intensity fluctuations (scintillations), which tend to reduce the energy fluence on target. In many cases, the turbulence limits the operational range and capability and may also results in system failure and temporary shutdown in strong turbulence conditions. Nevertheless, the effect of turbulence can be significantly reduced by adaptive optics (AO) techniques [4;5] even though many technical and physical challenges remain and the optimal designs are still to be found [6;7].

In this paper, we use a numerical simulation model to propagate the laser beam through turbulence for different turbulence conditions and ranges, and calculate the statistical variations of the fractional beam energy transmitted through a typical optical aperture of 10 cm. We also study the use of turbulence mitigation to improve beam delivery at the target. The simulations are applicable to a number of systems where it is important to maximize the pulse energy through an aperture, e.g. laser-based countermeasures, laser weapons, and free-space communication links. As an example, the results are applied to a high energy laser countermeasure system, where we determine the probability that a single laser pulse, or one of the pulses in a sequence, will provide a lethal energy inside the target aperture.

2. PRINCIPLES OF TURBULENCE MITIGATION

The phase and amplitude of a wave propagating through turbulence are affected in different ways: the phase gets distorted while the amplitude shows local fluctuations, as illustrated in Figure 1(a). If the conjugated wave, defined as the transformed wave with the conjugated phase and preserved amplitude, is sent back to its original position, the original phase and amplitude are restored at the initial position [5]. The conjugated wave is in fact pre-compensated for

Optics in Atmospheric Propagation and Adaptive Systems XVIII, edited by Karin U. Stein, John D. Gonglewski
Proc. of SPIE Vol. 9641, 96410B · © 2015 SPIE · CCC code: 0277-786X/15/$18 · doi: 10.1117/12.2194336

Downloaded From: https://www.spiedigitallibrary.org/conference-proceedings-of-spie on 03 Mar 2021
Terms of Use: https://www.spiedigitallibrary.org/terms-of-use

the turbulence to come. Wave conjugation is later on referred to as field conjugation. In practice, a laser beam is directed toward the target, as shown in Figure 1(a). A part of the beam hitting the target is reflected/scattered back toward the transmitter, and is used to probe the turbulence, as illustrated in Figure 1(b). The measured wave distortion is then used to pre-compensate the outgoing laser beam for turbulence, which focuses into a smaller spot at the target, as shown in Figure 1(c). This correction corresponds to either field- or phase conjugation (PC). With PC, the amplitude of the probing beam is disregarded. The phase of the probing beam is measured and applied to the outgoing beam with e.g. a Gaussian or top-hat amplitude profile. In this paper, turbulence mitigation is achieved with the help of PC.

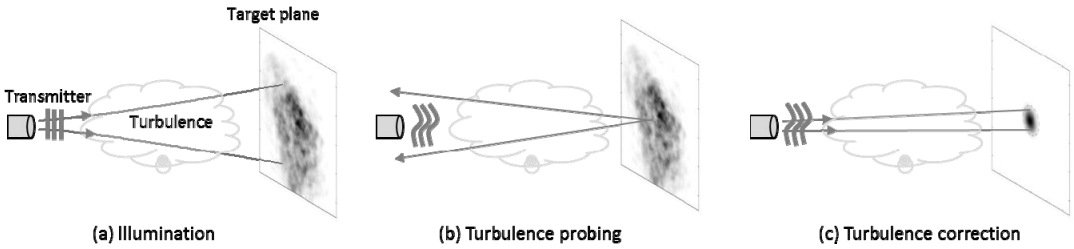

Figure 1. Turbulence mitigation principle for beam delivery improvement.

Turbulence correction is easier to perform in astronomical applications because turbulence can be probed by natural or artificial "guide stars", i.e. cooperative targets [8]. In addition, astronomers look at celestial bodies upwards, i.e. in a direction with favorable turbulence conditions. Beam delivery in military applications occurs, on the contrary, mostly along slant or near horizontal paths in strong turbulence conditions, with possibly a large apparent wind due to the platform speed, which requires correction of strong turbulence at high temporal bandwidths. These challenges need to be addressed appropriately in order to achieve satisfactory beam delivery improvement.

3. NUMERICAL SIMULATION MODEL

Beam propagation and turbulence correction simulations are performed with our numerical simulation model SISYFOS developed in-house at FFI [9]. It is based on the frozen atmosphere assumption and implemented with the help of the split-step-beam propagation method described elsewhere [10;11]. The simulation parameters used are shown in Table 1. The atmospheric path is momentarily modeled as a number of frozen phase screens (10 in this work) each described spatially by a Kolmogorov power spectrum, and the statistics of the turbulence is modeled by repeating the propagation simulation many times with other (statistically correct) sets of phase screens representing the chosen degree of turbulence, or alternatively modeling wind by laterally moving the phase screens. A multi-resolution grid includes the effect of the largest scale eddies through propagation. We here assume that the laser system is mounted on a platform with a speed of 50 m/s normal to the beam direction.

The rate at which the atmospheric turbulence varies is given by

$$\tau_{turb} = 0.314 \cdot \frac{r_0}{v}, \tag{1}$$

where r_0 is the Fried parameter [8], and v is the apparent wind speed. For a platform speed of 50 m/s, $C_n^2 = 10^{-13}\ m^{-2/3}$ and L=4000 m, τ_{turb} is calculated to be ~0.3 ms. The temporal resolution of the simulations τ_{res} is 0.1 ms, which is a factor of 3 shorter than the atmospheric time constant τ_{turb}.

Turbulence mitigation is achieved by applying phase conjugation (PC). "Ideal" AO correction in Table 1 corresponds to applying instantaneous PC at a frame rate of 10 kHz, i.e. $1/\tau_{res}$. We also tried to introduce a time delay of 0.5 and 1 ms, respectively, between probing and laser pulse propagation, which is longer than τ_{res}.

In the simulations, the laser beam is pointed toward the geometrical direction of the target located at the center of the grid. After propagation, the beam may partially miss the target due to beam wander, as illustrated in Figure 5. However, the long-term beam averaged over several realizations is centered on target. This implies that our simulations implicitly include a slow and coarse target tracking where image jitter is averaged out.

Downloaded From: https://www.spiedigitallibrary.org/conference-proceedings-of-spie on 03 Mar 2021
Terms of Use: https://www.spiedigitallibrary.org/terms-of-use

Table 1. Simulations parameters

Power spectrum	Kolmogorov. The inner and outer scales are equal to zero. In practice, they are given by the grid resolution and the grid size
Number of phase screens	10
Grid resolution	1 mm
Grid size	from 512 by 512 to 2048 by 2048 depending on the range and turbulence strength
Turbulence strength	$C_n^2 = 10^{-15}$, 10^{-14}, and 10^{-13} $m^{-2/3}$
Range	1000, 2000, and 4000 m
Temporal resolution τ_{res}	0.1 ms
Sequences	50 ms each (500 samples) through dynamic atmosphere (lateral wind)
Platform velocity	50 m/s

Turbulence mitigation	• No correction
	• AO correction: phase conjugation (PC)
	  ○ "ideal": 10 kHz
	  ○ 10 kHz and 0.5 ms delay
	  ○ 10 kHz and 1 ms delay

4. HIGH-ENERGY COUNTERMEASURES

As an example, we will apply the simulations to the case of a high-energy countermeasure (HECM) laser system, where the intention is to damage the focal plane sensor array (FPA) of an infrared missile seeker. This can be achieved by illuminating the seeker with a short and sufficiently intense laser pulse, or a sequence of such pulses. In order to be effective, the system should maximize the probability that a lethal pulse energy will hit inside the optical aperture of the seeker. This can be achieved in several ways:

- Increase the laser output energy: made possible by the recent advances in high-energy lasers.
- Decrease the laser divergence by using a wider output beam and/or improving beam quality.
- Use turbulence mitigation and tracking to improve beam delivery.
- Increase the number of launched pulses to increase the kill probability.

In this application, the intensity fluctuations induced by turbulence are of large interest because they determine whether a single pulse would hit the target with sufficient energy to destroy the sensor, or not. Answering that question requires a statistical approach, since turbulence is driven by stochastic processes. The occurrence probability of the energy hitting the target is determined later in this section with the help of numerical simulations.

4.1 Model parameters

The engagement scenarios are illustrated in Figure 2. A HECM laser beam at 4 μm is pointed and focused on an incoming missile. The laser pulse energy is assumed to be 0.1 J. A seeker tends to act as a retro-reflector for an incoming laser beam according to the cat-eye effect. The returned beam is used to probe the turbulence as described earlier in

Downloaded From: https://www.spiedigitallibrary.org/conference-proceedings-of-spie on 03 Mar 2021
Terms of Use: https://www.spiedigitallibrary.org/terms-of-use

Section 2. The HECM laser aperture should be small to limit interactions with the platform (e.g. drag, aero-optical effects). At the same time, a larger beam at the transmitter can be focused into a smaller spot on target, thereby increasing the energy fluence. As a compromise, we chose the laser output aperture to be 15 cm in diameter. The beam waist radius ω_0 of the outgoing laser beam is chosen to be 54 mm, and the beam quality M^2=1, resulting in 98% transmission through the 15 cm diameter aperture and a total beam divergence of 48 μrad (FW1/e^2M). A laser beam quality of M^2 =2 is easier to achieve and therefore interesting to include in our simulations. Modeling such a beam is however not straightforward since there is indeed an infinite number of phase profiles with an M^2-value of 2. In order to bypass this problem, we model an outgoing beam with a $\omega_0/2$ waist radius to emulate a beam with a factor of 2 larger divergence. This is obviously not completely representative for a M^2 =2 beam, as this beam experiences less turbulence close to the platform due to its smaller size. However, for propagation over 1000 m and for high turbulence levels, this approximation is quite adequate. Later in this paper, we refer to the two different laser beams as M^2 =1 and M^2 =2 beams, respectively (see Figure 3).

The platform carrying the HECM is assumed to fly at a velocity of 50 m/s, which corresponds to the typical velocity of a transport helicopter. In our model, the incoming missile is located 1000 m, 2000 m, or 4000 m away, respectively.

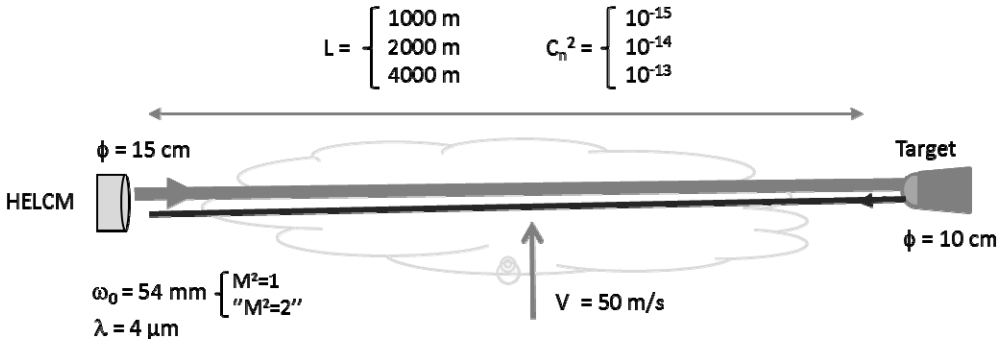

Figure 2. Engagement scenarios.

We assume that the missile seeker has an optical aperture of 100 mm and a sensor pixel size of 30 μm (see Table 2). The energy hitting the seeker is focused into a small spot on the sensor, roughly the size of a pixel. At the FPA, the delivered energy fluence averaged over a pixel is

$$F = \frac{EIB \cdot E_{out} \cdot T}{pix^2}, \tag{2}$$

where E_{out} is the laser pulse energy, T is the seeker optics transmission, pix is the array pitch size, and EIB is the fractional energy-in-bucket (pulse energy hitting the seeker aperture) relative to the laser output pulse energy E_{out}. The laser-induced damage threshold for sensor materials can vary by orders of magnitude, from very low values to more than 1 J/cm^2. Disabling a substantial part of the sensor presumably requires an energy fluence orders of magnitude larger. For the sake of our demonstration, we assume that the lethal fluence F_{lethal} for the sensor (and thus the missile) is 10^3 J/cm^2. This would probably disable the sensor over a large spot including numerous pixels, and the damage could be extended to several spots by illumination with a sequence of several pulses. Given a 0.1 J laser pulse output, the lethal fluence level of 10^3 J/cm^2 is reached for an EIB value of 20%, that is 20 mJ energy hitting the seeker aperture.

Table 2. Seeker characteristics.

Aperture	100 mm
Pixel size, *pix*	30 μm
Transmission, *T*	50%
Lethal fluence, F_{lethal}	10^3 J/cm^2

Downloaded From: https://www.spiedigitallibrary.org/conference-proceedings-of-spie on 03 Mar 2021
Terms of Use: https://www.spiedigitallibrary.org/terms-of-use

4.2 Simulations

Figure 3 shows the long-term beam size of focused beams at different distances and increasing turbulence conditions, calculated from the analytic expressions given in [12]. At $C_n^2=10^{-15}$ $m^{-2/3}$, the turbulence is weak and the beam is focused into a diffraction limited spot. The arrow on the left hand side of Figure 3 shows the target aperture (10 cm diameter). The beam size of the $M^2=2$ beam is twice as large as the $M^2=1$ beam due to its twice as large divergence. The long-term beam size at the target gets larger due to beam spread and beam wander, as the turbulence increases. Interestingly, the difference in beam size between the $M^2=2$ and the $M^2=1$ beams are decreasing, and are indeed quite similar at $C_n^2=10^{-13}$ $m^{-2/3}$. In the strong turbulence regime, beam spread becomes indeed dominant and the divergence of the beam depends no longer on its initial size.

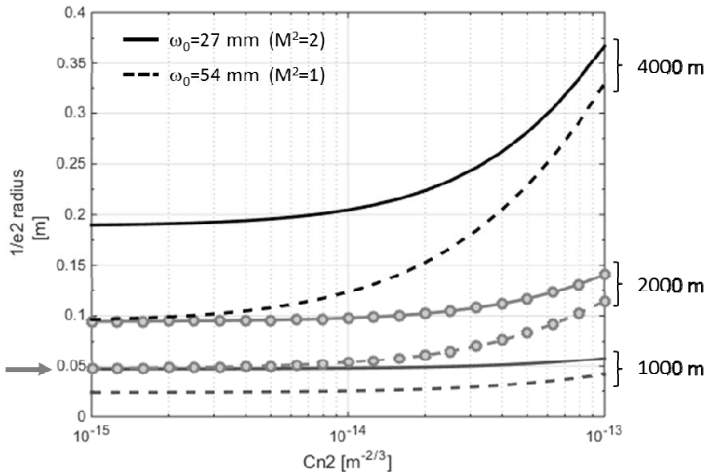

Figure 3. Long-term $1/e^2$ beam radius at target (1000, 2000 and 4000 m distance, respectively) for increasing turbulence.

From the long-term beam size data presented in Figure 3, we deduce the amount of energy hitting the 100 mm target aperture, called the long-term Energy-In-Bucket <EIB>, as illustrated in Figure 4. <EIB> is normalized by the pulse energy of the outgoing beam: <EIB>=100% means that the whole beam hits the target aperture. The diffraction limited (no turbulence case) <EIB> is lower with the $M^2=2$ beam because the beam at the target is larger. As mentioned above, at 4000 m distance and $C_n^2=10^{-13}$ $m^{-2/3}$, the $M^2=2$ and the $M^2=1$ beams are similar in size and <EIB>. The circles show the simulation results (snap-shots averaged over several realizations of 50 ms time periods) that are in good agreement with the analytic theory. Examples of snap-shots are shown in Figure 5. They show that, as the turbulence increases, the short-term beam gets wider due to beam spread, and misses partly or fully the target due to beam wander. In strong turbulence regime, the beam spread is large and hot spots appear.

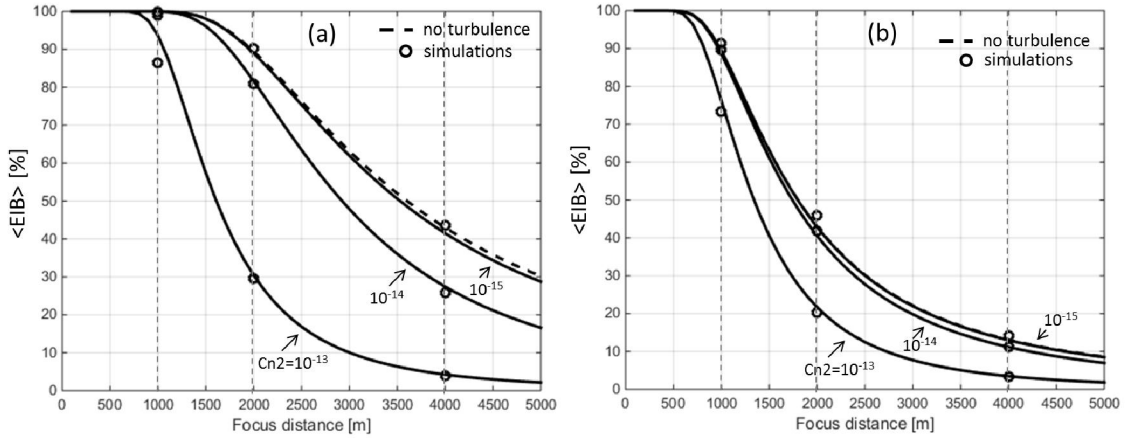

Figure 4. Normalized <EIB> hitting the target for beam quality (a) $M^2=1$ and (b) $M^2=2$. The solid and dashed lines show the analytical value of <EIB> in different turbulence conditions, and without turbulence (diffraction limited), respectively. The empty circles show the results of the numerical simulations.

Downloaded From: https://www.spiedigitallibrary.org/conference-proceedings-of-spie on 03 Mar 2021
Terms of Use: https://www.spiedigitallibrary.org/terms-of-use

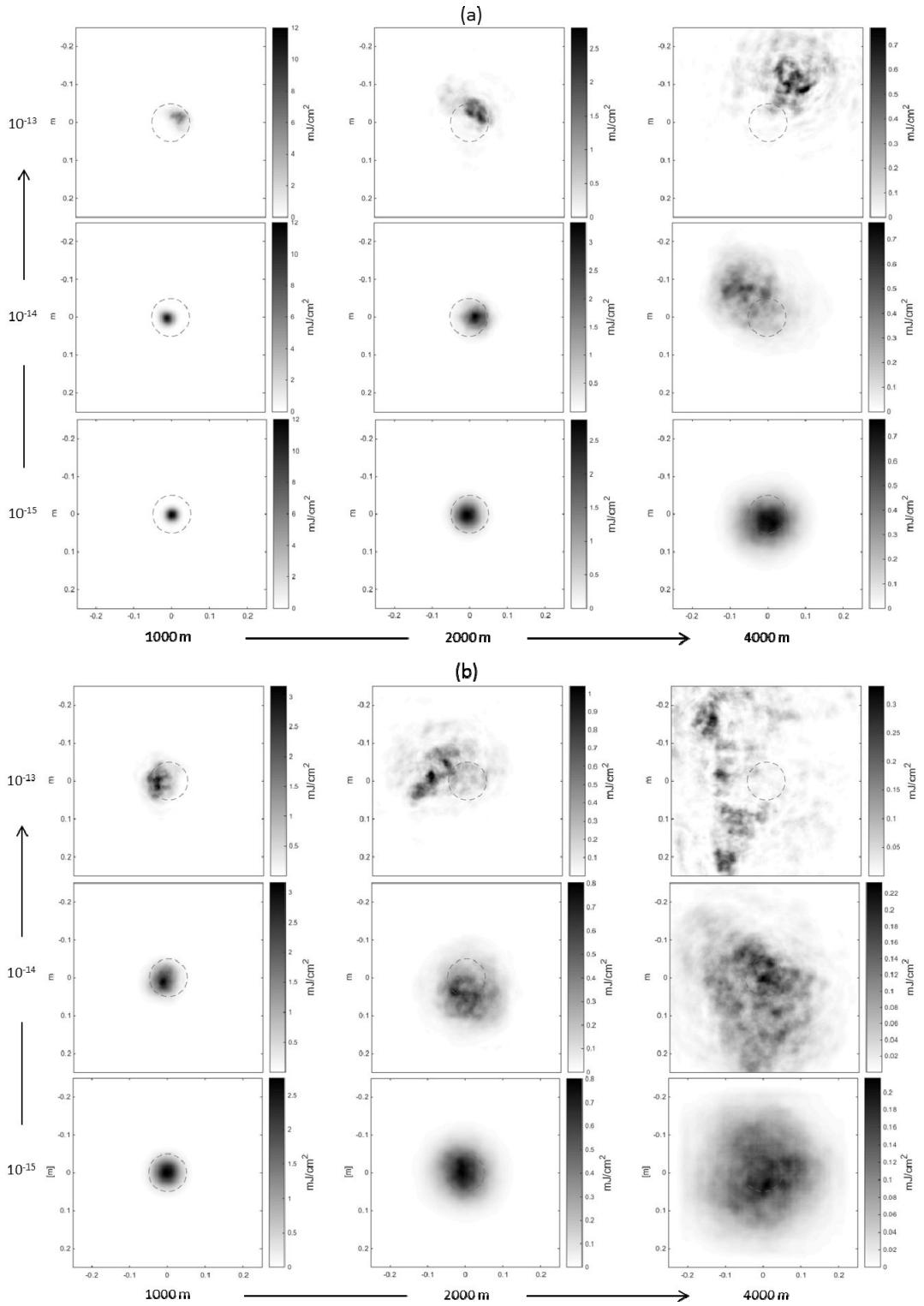

Figure 5. Snap-shot simulations of the laser beam at 1000, 2000, and 4000 m distance respectively. Snap-shots are shown for $C_n^2 = 10^{-15}$, 10^{-14} and 10^{-13} $m^{-2/3}$, respectively. The dotted line shows the target aperture (10 cm diameter). The outgoing beam has a pulse energy of 0.1 J. Note that the energy fluence scale is different at 1000, 2000 and 4000 m. The beam quality is (a) $M^2 = 1$ and (b) $M^2 = 2$.

Downloaded From: https://www.spiedigitallibrary.org/conference-proceedings-of-spie on 03 Mar 2021
Terms of Use: https://www.spiedigitallibrary.org/terms-of-use

Figure 6 illustrates the benefit of AO correction: the initial EIB is increased from 13% to 65% with PC.

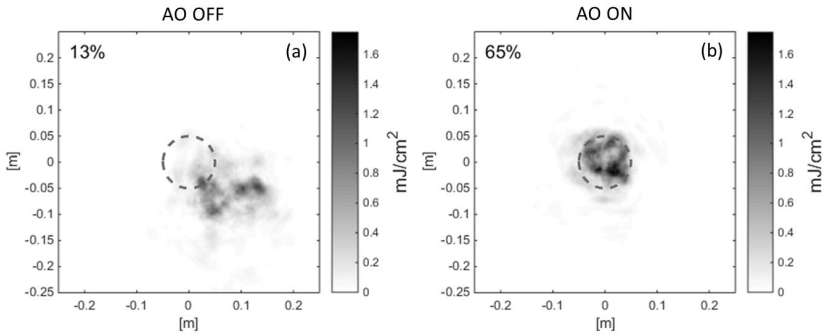

Figure 6. Snap-shot simulations for L=2000 m, $C_n^2 = 10^{-13}$ $m^{-2/3}$ and beam quality $M^2 = 1$: (a) no correction, (b) "ideal AO correction" (PC). The EIB is 13% and 65%, respectively. The outgoing beam has a pulse energy of 0.1 J.

4.3 Analysis method

The EIB is calculated from the simulation data for the different sets of distances, turbulence strengths and turbulence mitigation parameters, as illustrated in Figure 7. On the left hand side, we show the EIB for ten realizations of 50 ms long sequences. The solid and dashed grey lines show the mean value and the 95% confidence interval, respectively. From the EIB time series, we calculate the mean <EIB> and the normalized standard deviation σ_{nEIB} defined as:

$$\sigma_{nEIB} = \frac{\sigma_{EIB}}{\langle EIB \rangle}. \tag{3}$$

The parameters <EIB> and σ_{nEIB} are used in the Section 4.4 to characterize the performance of the different turbulence mitigation parameters. From the EIB time series we derive the occurrence probability of EIB, as illustrated on the right hand side in Figure 7. Occurrence probability reflects the stochastic nature of turbulence and is the basis for the analysis carried out in Section 4.5 that handles the kill probability of the missile.

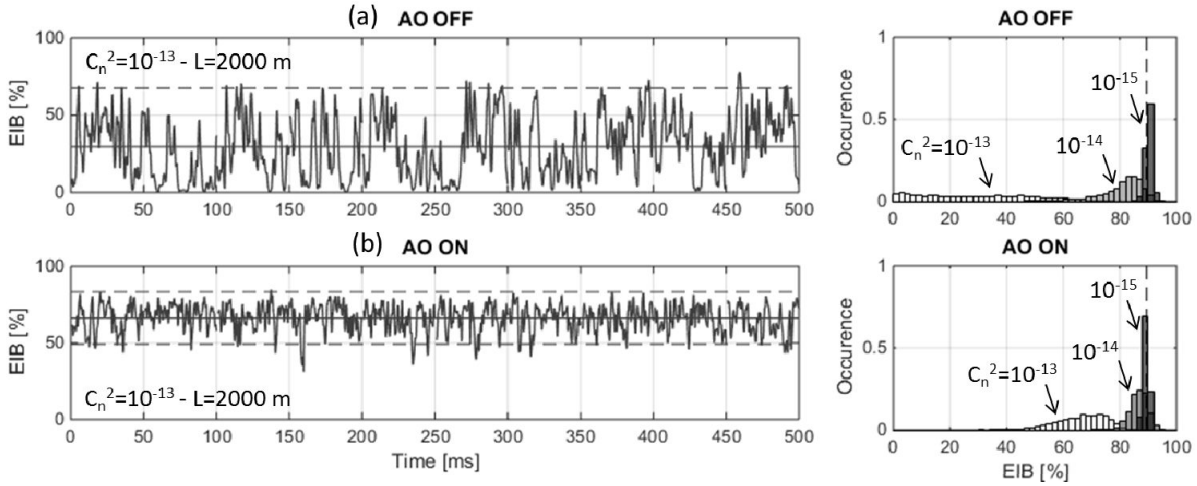

Figure 7. Left hand size: EIB for L=2000 m, $C_n^2 = 10^{-13}$ $m^{-2/3}$ and beam quality $M^2 = 1$. The solid and dashed lines show <EIB> and the 95% confidence interval, respectively. Right hand side: occurrence probability of EIB. The dashed lines show the diffraction limit (no turbulence case). (a) no correction, and (b) AO correction (PC).

Downloaded From: https://www.spiedigitallibrary.org/conference-proceedings-of-spie on 03 Mar 2021
Terms of Use: https://www.spiedigitallibrary.org/terms-of-use

4.4 Performance of turbulence mitigation

In Table 3, we show a list of the different correction methods evaluated in this work. The numbers will be used as references in figures presented below.

Table 3. Series numbers referring to the different turbulence mitigation methods (used later in figures).

Series numbers	Description
"**1**"	No correction
"**2**"	"Ideal" AO correction (PC) 10 kHz
"**3**"	AO correction (PC) 10 kHz, 0.5 ms delay
"**4**"	AO correction (PC) 10 kHz, 1 ms delay

The parameters <EIB> and σ_{nEIB} are plotted against each other in Figure 8 and Figure 9 for the whole sets of simulations carried out (see Table 3), for M^2=1 and M^2=2, respectively. Turbulence correction tends to increase <EIB> and decrease σ_{nEIB}, which comes out in the coordinate system (<EIB>, σ_{nEIB}) by a displacement toward the lower right hand corner. The "ideal" AO correction "2" gives the upper bound limit of performance. Further, no correction "1" gives the lower bound limit of performance. Those bound limits of performance are highlighted by dotted lines connecting points "1" and "2". The vertical dashed lines show EIB without turbulence (i.e. diffraction limited) determined in Figure 4. Note that the diffraction limit does not represent an absolute limit for <EIB>. Indeed, beam wander correction using e.g. tracking reduces the beam size at target and can increase <EIB> somewhat beyond this value, which would be noticeable whenever beam wander is dominant, typically for low turbulence level combined with longer distances, for example for $C_n^2=10^{-15}$ $m^{-2/3}$ and L=4000 m.

Next, we look at the sequences with the lowest turbulence strength, $C_n^2=10^{-15}$ $m^{-2/3}$, marked by diamonds: turbulence is negligible and no turbulence mitigation of any kind is required. Obviously and generally speaking, there is not necessarily a need for correction whenever σ_{nEIB} is already low without correction. Indeed an EIB increase of 15-20% will hardly justify the integration of a turbulence correction system in a high-energy-laser application. It is probably easier to increase the output power by 15-20% instead. We set the boundary for σ_{nEIB} to 10^{-1}, as shown by the horizontal dashed lines. Values under this boundary are disregarded because no turbulence correction is needed. This leaves us with three interesting cases highlighted by stars. In Figure 8(b), ($C_n^2=10^{-13}$ $m^{-2/3}$ and L=2000 m), the outer limits of performance (between "1" and "2") show a <EIB> gain factor of more than 2, whereas σ_{nEIB} is divided by a factor 5. This is a significant improvement. Gain performance is reduced by roughly a factor 2 with AO 0.5 ms delay "3". Next, in Figure 8(c), ($C_n^2=10^{-13}$ $m^{-2/3}$ and L=4000 m), the <EIB> gain between "1" and "2" is larger than 4 and σ_{nEIB} is divided by 2, while AO 0.5 ms delay gives quite bad performance. Finally, at $C_n^2=10^{-14}$ $m^{-2/3}$ and L=4000 m in Figure 8(c), the <EIB> gain is 1.6 and σ_{nEIB} is divided by 2. In this case, AO "2" and AO 0.5 ms delay "3" performs almost equally.

Figure 9 shows σ_{nEIB} against <EIB> for the laser with beam quality M^2=2. In this case, the beam is twice as divergent and is therefore focused into a larger spot, as shown by the diffraction limits in Figure 8 and Figure 9. At $C_n^2=10^{-13}$ $m^{-2/3}$ and L=2000 m, the <EIB> gain is 1.7 while σ_{nEIB} is divided by 1.8. At $C_n^2=10^{-13}$ $m^{-2/3}$ and L=4000 m (see Figure 9(c)), Finally, at $C_n^2=10^{-14}$ $m^{-2/3}$ and L=4000 m, the <EIB> gain is only 1.3 while σ_{nEIB} keeps stable. These results are summarized in Figure 10 that shows the gain in <EIB> and σ_{nEIB} for the AO correction "2" and "3".

Downloaded From: https://www.spiedigitallibrary.org/conference-proceedings-of-spie on 03 Mar 2021
Terms of Use: https://www.spiedigitallibrary.org/terms-of-use

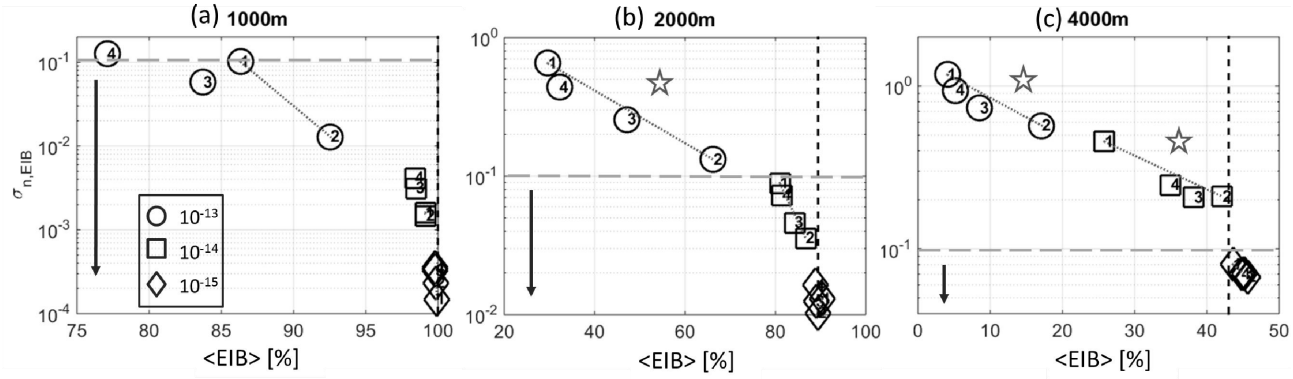

Figure 8. σ_{nEIB} against <EIB> for turbulence corrections listed in Table 3 for different turbulence conditions and beam quality M^2=1 for (a) L=1000 m, (b) L=2000 m, and (c) L=4000 m. The dotted lines between "1" and "2" highlight the bound limit of performance. The horizontal and vertical dashed lines show the 10^{-1} threshold value of σ_{nEIB} and the value of <EIB> without turbulence (diffraction limit), respectively. The stars highlight the cases of interest.

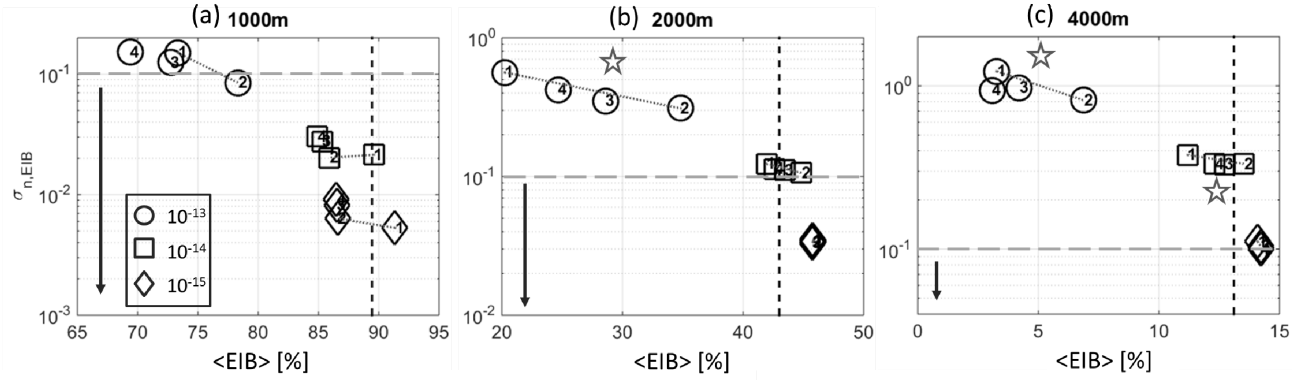

Figure 9. σ_{nEIB} against <EIB> for turbulence corrections listed in Table 3 for different turbulence conditions and beam quality M^2=2 for (a) L=1000 m, (b) L=2000 m and, (c) L=4000 m.The dotted lines between "1" and "2" highlight the bound limit of performance. The horizontal and vertical dashed lines show the 10^{-1} threshold value of σ_{nEIB} and the value of <EIB> without turbulence (diffraction limit), respectively. The stars highlight the cases of interest.

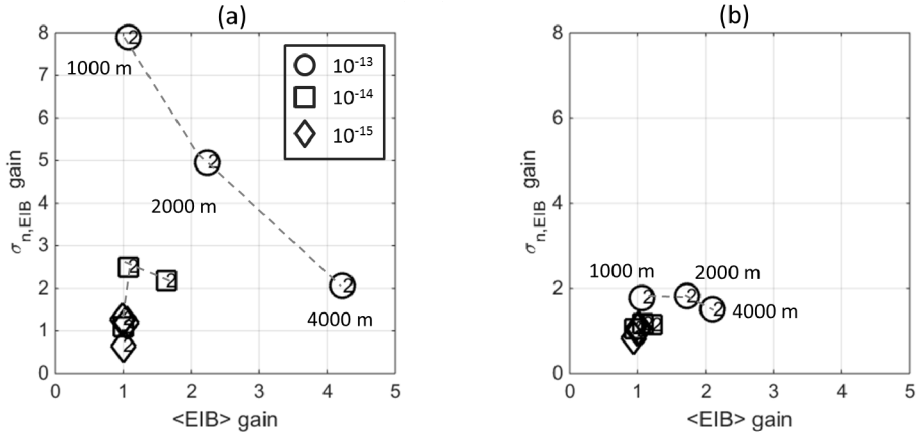

Figure 10. Performance of turbulence mitigation for beam with beam quality (a) M^2=1, and (b) M^2=2.

Downloaded From: https://www.spiedigitallibrary.org/conference-proceedings-of-spie on 03 Mar 2021
Terms of Use: https://www.spiedigitallibrary.org/terms-of-use

To sum up, beam delivery benefits from turbulence mitigation in terms of <EIB> increase and intensity fluctuations decrease. However, correction has to be applied at high rates larger than $1/\tau_{turb}$, where τ_{turb} is the turbulence time scale defined by Eq.1 ($\tau_{turb} \geq 0.3$ ms in this scenario), and time delay has to be minimized. This is a challenge for long propagation paths in strong turbulence, and particularly for high-velocity platforms. The best performance improvement is obviously achieved with the M^2=1 beam due to its intrinsic nature to focus into a smaller spot. This is especially manifested when beams are focused 4000 m away through strong turbulence $C_n^2 = 10^{-13}$ $m^{-2/3}$. Both M^2=1 and M^2=2 beams have a similar long-term size (hence <EIB>), but AO correction performs nevertheless better for M^2=1.

As the turbulence increases and beam spread gets very large, the beam gets dislocated, PC fails to counteract turbulence equally well, and performance saturates and drops, i.e. less energy is concentrated on target. In this turbulence regime turbulence-induced hot spots also appear, with intensity levels possibly several times larger than those obtained at the diffraction limit, and size similar to the coherence length ρ_0 [12]. In Figure 11(b), we show a snapshot of the beam at target when no correction is applied. The beam is spread and dislocated and a hot spot appears. The energy fluence of the hot spot is in fact ten times larger than the diffraction limited fluence shown in Figure 11(a). The hot spot "misses" however the target, resulting in a small EIB value (6%). Next in Figure 11(c), adaptive optics (PC) concentrates the beam to some extent and increases the EIB from 6% to 11%, but yet leads to the extinction of the hot spot. Turbulence correction does indeed not necessarily lead to the optimization of the spot brightness, as discussed by Vorontsov et al. [5]. In Figure 11(d), the seeker aperture is artificially centered at the hot spot location, increasing the EIB value to 30%, largely exceeding the diffraction limited EIB value of 14%. This shows the large amount of energy contained in hot spots. Hot spots hit occasionally the target aperture resulting in high EIB exceeding the diffraction limit. Such happenings contribute to increase the kill probability, as discussed in Section 4.5.

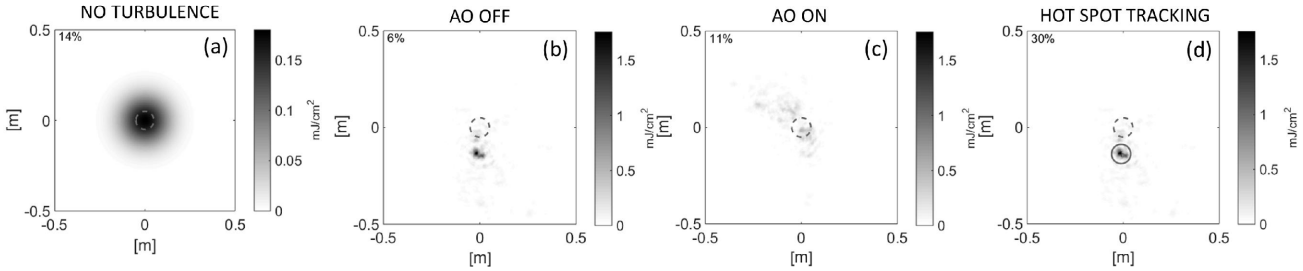

Figure 11. Snap-shot simulation for L=4000 m, $C_n^2 = 10^{-13}$ $m^{-2/3}$, and beam quality M^2 =2 in case of (a) no turbulence, (b) no correction, (c) "ideal" AO correction (PC) 10 kHz, and (d) Artificial hot spot tracking. The outgoing laser pulse has an energy of 0.1 J. Note that the fluence scale is ten times smaller in (a) than in (b), (c), and (d).

4.5 Kill probability assessment

Our statistical analysis is based on the occurrence probability of EIB for a single pulse, presented in Section 4.3, and illustrated in Figure 12(a). The occurrence probability gives the probability for a single laser pulse to hit the target with a given EIB. From this we can calculate p_{min}, defined as the probability for a single pulse to hit the target with an EIB-value of EIB_{min} or larger, as shown in Figure 12(b) for L=4000 m. As an example, for $C_n^2 = 10^{-14}$ $m^{-2/3}$ and no correction, the probability that the single pulse EIB is larger than 20% is 0.65. This probability increases to 1 with PC correction.

Now, to increase the occurrence probability of higher EIBs, we can consider launching a short train of pulses instead. For each pulse, the probability is p_{min} that the pulse energy exceeds a given EIB. There are two events: namely under/above a given EIB, and the probability $P(k,n)$ that k pulses out of n are above that threshold is given by the binomial distribution:

$$P(k,n) = \frac{n!}{k!(n-k)!} \cdot p_{\min}^{k} \left(1 - p_{\min}\right)^{n-k} \cdot \tag{4}$$

Finally the probability that <u>at least</u> k pulses out of n are above threshold is given by

$$p(k,n) = \sum_{k}^{n} P(k,n) \cdot \tag{5}$$

Downloaded From: https://www.spiedigitallibrary.org/conference-proceedings-of-spie on 03 Mar 2021
Terms of Use: https://www.spiedigitallibrary.org/terms-of-use

For k=1, $p(k,n)$ simplifies to

$$p(1,n) = 1-(1-p_{\min})^n \cdot \tag{6}$$

The occurrence probability $p(1,10)$ that at least 1 out of 10 pulses is above threshold is shown in Figure 12(c) and Figure 13(c) for M^2 =1 and M^2 =2-beams, respectively. By allowing 10 pulses to be launched, the probability that one of the pulses exceeds a given EIB level increases significantly. Also shown in Figure 12-13(d) is the occurrence probability $p(10,20)$. Then, we determine the minimum energy level EIB_{min} hitting the target with a 98% probability for a single pulse, 1/10 pulses and 10/20 pulses, respectively. The results are marked with empty circles in Figure 12-13, and reported into Figure 14. In this figure, the lowest symbols show the EIB without AO correction, and the upper symbol the EIB with AO correction. In section 4.1, we assumed the lethal fluence to be 10^3 J/cm^2 corresponding to an EIB value of 20%, that is 20 mJ hitting the seeker aperture for a laser pulse output of 0.1 J. For L=1000 and 2000 m, the energy fluence on target with AO correction exceeds the lethal fluence except for the M^2=2 single pulse case at $C_n^2=10^{-13}$ m$^{-2/3}$ (see Figure 14). It is emphasized that turbulence mitigation is however very efficient as the minimum energy fluence at target is multiplied by a factor 10 and 30, for M^2=2 and M^2=1, respectively. This corresponds to an increase of the kill probability from 47 to 93% and from 63 to 100%, respectively, as shown in Figure 15. For L=4000 m, the gain factor in fluence is still over 20 for M^2=1 in the strong turbulence conditions. In this case, the kill probability is increased from 1.6 % to 35% for a single pulse and up to 100% with a train of 10 pulses.

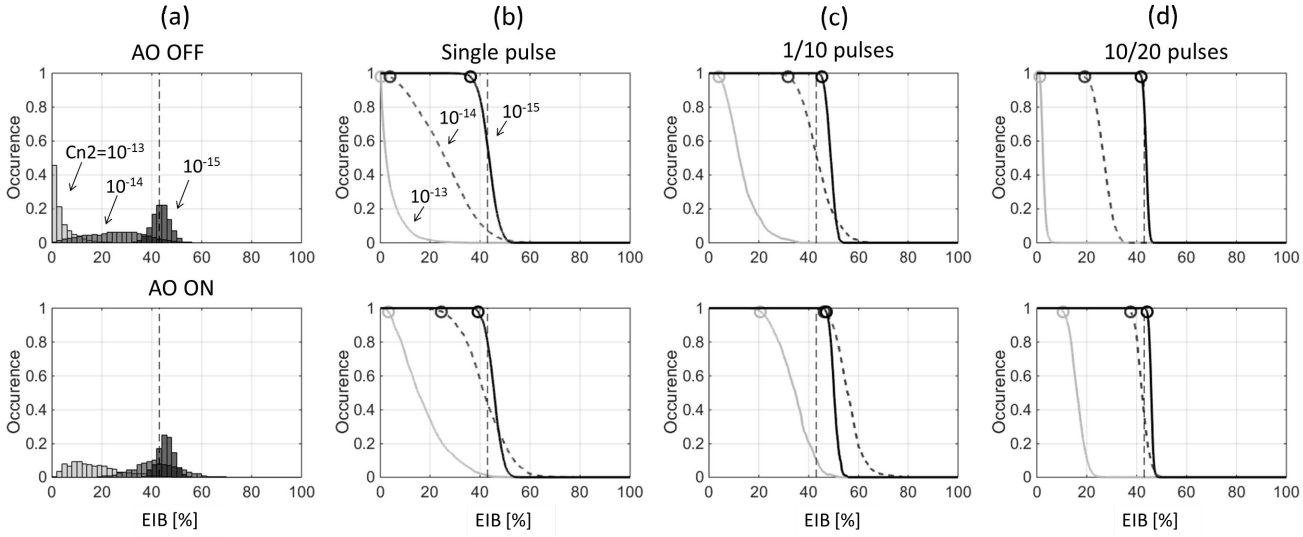

Figure 12. L=4000 m and beam quality M^2 =1, no correction "1", AO correction "2": (a) occurrence probability of EIB for a single pulse, (b) occurrence probability that a single pulse exceeds a given EIB-value, (c) occurrence probability that at least 1 pulse out of 10 exceeds a given EIB-value, and (d) occurrence probability that a least 10 pulses out of 20 exceed a given EIB-value. The dashed lines show the EIB for a diffraction limited beam, and the empty circles the minimum EIB with 98% probability.

Downloaded From: https://www.spiedigitallibrary.org/conference-proceedings-of-spie on 03 Mar 2021
Terms of Use: https://www.spiedigitallibrary.org/terms-of-use

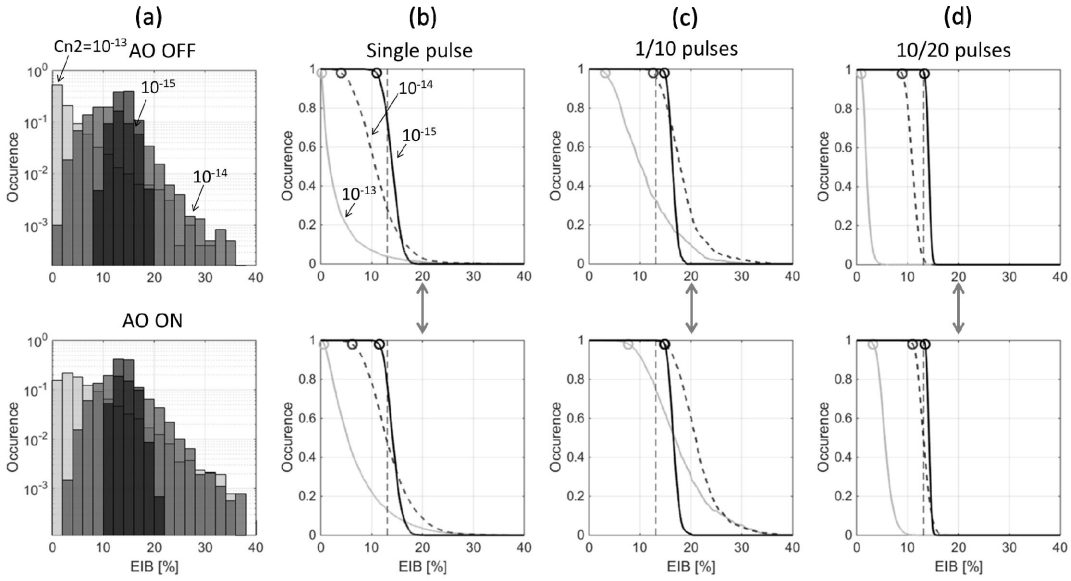

Figure 13. L=4000 m and beam quality M^2 =2, no correction "1", AO correction "2": (a) occurrence probability of EIB for a single pulse, (b) occurrence probability that a single pulse exceeds a given EIB-value, (c) occurrence probability that at least 1 pulse out of 10 exceeds a given EIB-value, and (d) occurrence probability that a least 10 pulses out of 20 exceed a given EIB-value. The dashed lines show the EIB for a diffraction limited beam, and the empty circles the minimum EIB with 98% probability. The double-arrows show the 20% EIB-value corresponding to the lethal fluence of 10^3 J/cm^2.

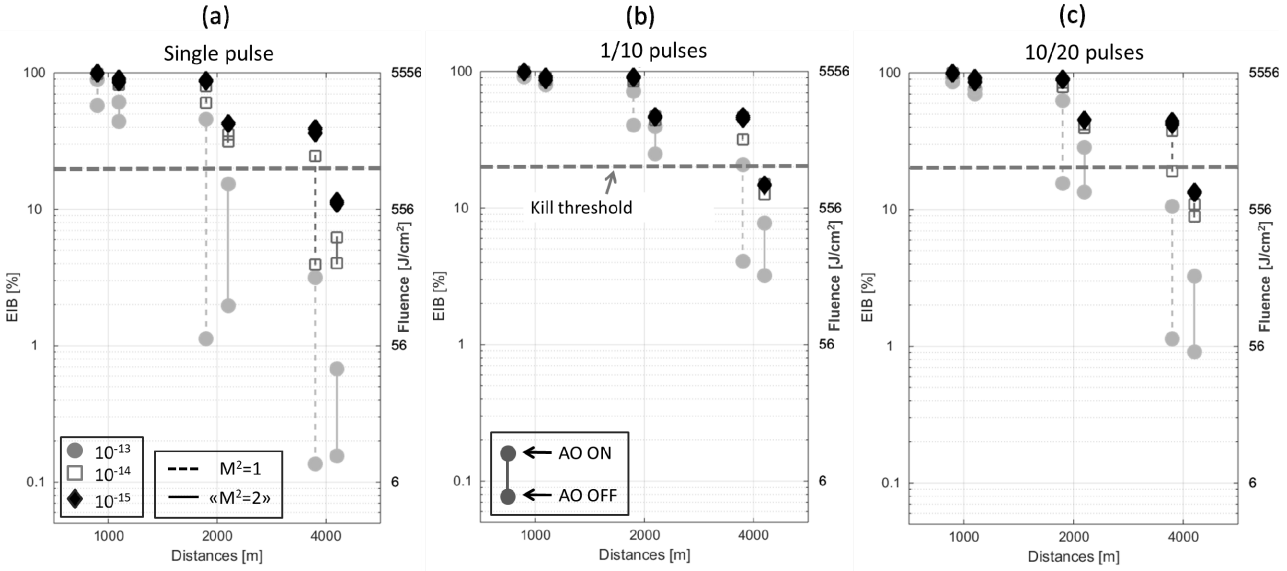

Figure 14. Minimum EIB/energy fluence at target FPA with 98% probability for no correction "1" (lower symbol) and AO correction "2" (upper symbol), at 1000, 2000 and 4000 m distances, respectively, for (a) a single pulse, (b) at least 1 pulse out of 10, and (c) at least 10 pulses out of 20. We assume a laser with 0.1 J energy pulse output. The arrow shows the lethal fluence F_{lethal} at 10^3 J/cm^2 equivalent to 20% EIB.

The kill probability presented in Figure 15 also shows some remarkable results. Noticeably, for M^2=2, the kill probability for 1/10 pulses is down to zero for C_n^2=10^{-15} m$^{-2/3}$, but as high as 30% and 60% in stronger turbulence conditions. In other words, turbulence contributes somewhat surprisingly to increase the kill probability. This effect is due to turbulence-induced intensity fluctuations that exceed the fluence for the diffraction limited beam, which occurs

Downloaded From: https://www.spiedigitallibrary.org/conference-proceedings-of-spie on 03 Mar 2021
Terms of Use: https://www.spiedigitallibrary.org/terms-of-use

occasionally whenever a hot spot hits the seeker aperture, as commented earlier in section 4.4 and illustrated in Figure 11. Note that this effect occurs without AO correction, but is however enhanced with AO correction. In Figure 13(a), the upper EIB-values are indeed higher for $C_n^2=10^{-13}$ and 10^{-14} $m^{-2/3}$ than in weaker turbulence for $C_n^2=10^{-15}$ $m^{-2/3}$ due to "wings" in the occurrence probability. This has obviously an impact on the occurrence probability for a single or several pulses of hitting the target with a given energy fluence. The most obvious case is shown in Figure 13(c) with AO correction. In this case, the occurrence probability is always higher for $C_n^2=10^{-14}$ $m^{-2/3}$ than for weaker turbulence $C_n^2=10^{-15}$ $m^{-2/3}$ (the dashed curve stays always above the solid black curve). For EIB=20% (marked by the double arrows), the occurrence probability is 0% and 60% for 10^{-15} $m^{-2/3}$ and 10^{-14} $m^{-2/3}$, respectively.

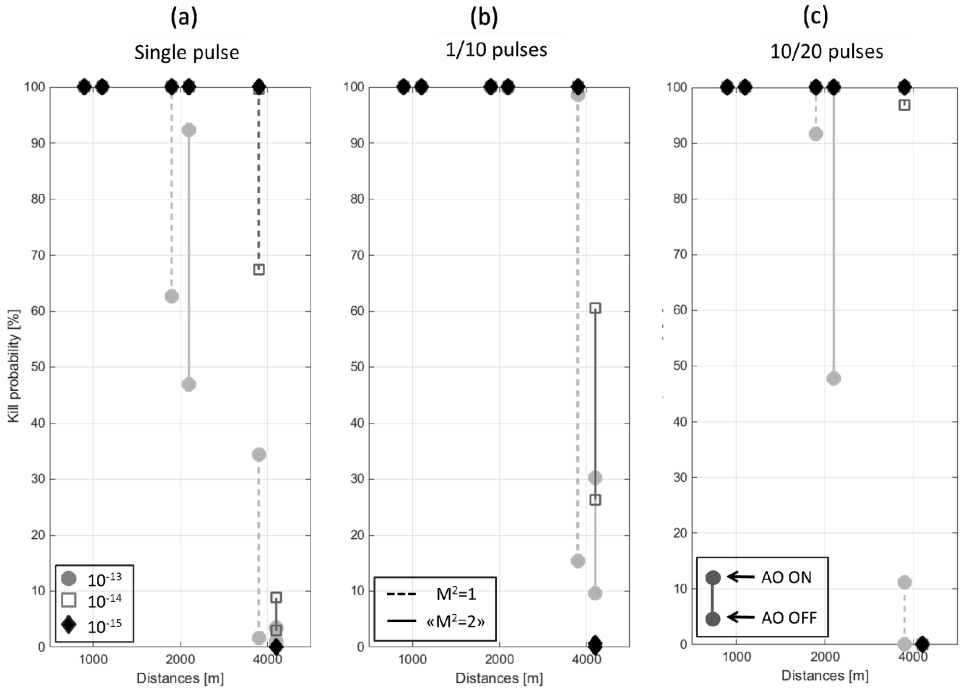

Figure 15. Kill probability for EIB=20% i.e. a lethal fluence of 10^3 J/cm^2 and 0.1 J energy pulse output for (a) a single pulse, (b) at least 1 pulse out of 10, and (c) at least 10 pulses out of 20.

5. CONCLUSIONS AND FUTURE WORK

This paper shows that turbulence mitigation performs well even at large ranges and under strong turbulence conditions, and results in a significant increase of the kill probability. The best improvements are achieved for a diffraction limited beam ($M^2=1$) that can potentially focus into a smaller spot on the target. The loss of energy due to larger divergence-beams can however be compensated by increasing the laser pulse energy. Alternatively, launching a small train of pulses instead of a single pulse can also contribute significantly to improve the kill probability. We have also demonstrated that for some special conditions, the kill probability is higher with stronger turbulence. In this case, the turbulence is indeed beneficial because it can lead to hot spots hitting the target aperture.

In the future, high-energy countermeasures are likely to include turbulence correction in order to be operational in harsh conditions and over long-distances. However, many challenges are still to be addressed. Tracking and turbulence correction must operate at very high speeds with iteration rates of tens of kHz to handle the rapid fluctuations induced by the apparent wind on high-velocity platforms

Finally, the present simulations did not include plumes, rotor down-wash and aero-optical effects that are likely to significantly increase the amount of turbulence, and set higher requirements to the system. Field conjugation was not addressed in this paper. Simulations show that field conjugation can further improve the performance [5]. Field conjugation can also be integrated in our numerical model, as well as an extended laser model including the laser pulse temporal and spatial behavior.

Downloaded From: https://www.spiedigitallibrary.org/conference-proceedings-of-spie on 03 Mar 2021
Terms of Use: https://www.spiedigitallibrary.org/terms-of-use

REFERENCES

[1] G. P. Perram, S. J. Cusumano, R. L. engehold, and S. T. Fiorino, “An introduction to laser weapon systems,” Directed Energy Professional Society, (2010).

[2] G. C. Manke II, "Lasers in Electronic Warfare," Proc. SPIE 9251, (2014).

[3] F. Moll, C. Fuchs, and J. Horwath, "Laser communication between fast-flying platform and ground station," SPIE Newsroom, (2015).

[4] T. Weyrauch and M. A. Vorontsov, "Atmospheric compensation with a speckle beacon in strong scintillation conditions:directed energy and laser communication applications," Appl. Optics, 44(30), 6388-6401 (2005).

[5] M. A. Vorontsov, V. V. Kolosov, and A. Kohnle, "Adaptive laser beam projection on an extended target: phase- and field-conjugate precompensation," J. Opt. Soc. Am. A, 24(7), 1975-1993 (2007).

[6] M. A. Vorontsov, V. V. Kolosov, and E. Polnau, "Target-in-the-loop wavefront sensing and control with a Collett-Wolf beacon: speckle-average phase conjugation," Appl. Optics, 48(1), 13-29 (2009).

[7] A. Khizhnyak, V. Markov, J. Chavez, and S. Liu, "Beacon-defined performance in adaptive optics," Proc. SPIE, 8517, (2012).

[8] R. K. Tyson, “Principles of adaptive optics*,”* Boston: Academic Press, (1998).

[9] G. Arisholm, "Quantum noise initiation and macroscopic fluctuations in optical parametric oscillators," J. Opt. Soc. Am. B, 16(1), 117-127 (1999).

[10] A. Belmonte, "Feasibility study for the simulation of beam propagation: consideration of coherent lidar performance," Appl. Optics, 39(30), 5426-5444 (2000).

[11] M. Carbillet, C. Verinaud, B. Femenia, A. Riccardi, and L. Fini, "Modelling astronomical adaptive optics - I. The software package CAOS," Mon. Not. R. Astron. Soc., 356, 1263-1275 (2005).

[12] L. C. Andrews and R. L. Phillips, “Laser beam propagation through random media, second edition. Bellingham,” Washington: SPIE Optical Engineering Press, (2005).

Downloaded From: https://www.spiedigitallibrary.org/conference-proceedings-of-spie on 03 Mar 2021
Terms of Use: https://www.spiedigitallibrary.org/terms-of-use